Structural Studies on a Ribonucleoprotein Organelle: The Ribosome

A. YONATH[1]

1 Introduction

One of the most abundant cellular assemblies of RNA and proteins is the ribosome, the organelle which operates as a multi-functional enzyme translating the genetic code into polypeptide chains. Ribosomes are built of two structurally independent subunits of unequal size, which associate upon initiation of protein biosynthesis. A typical bacterial ribosome contains about a quarter of a million atoms and is of a molecular weight of approximately 2.3 million daltons. About two-thirds of its mass is comprised of three chains of rRNA, the rest includes some 57 different proteins.

Results of intensive biochemical, biophysical and genetic studies illuminated several functional aspects of the process of protein biosynthesis and led to suggestions (1) for the overall shape and the quaternary structure of the ribosome; (2) for the spatial proximities of various ribosomal components; (3) for the secondary structure of ribosomal RNA chains; and (4) for the approximate positioning of several reaction sites. Accumulated evidence has decisively shown that the ribosomal RNA is not only scaffolding the ribosomal proteins but has significant functional and enzymatic roles in facilitating the peptidyl-transferase reaction. However, the understanding of the molecular mechanism of protein biosynthesis is still hampered by the lack of a molecular model.

This chapter describes the recent advances in crystallography and image reconstruction of intact, complexed and modified ribosomal particles. Highlighted are the results which stimulated new biochemical and structural experiments. Of particular interest is the design of crystalline complexes suitable for investigations of functional and dynamic aspects of protein biosynthesis.

[1] Department of Structural Chemistry, Weizmann Institute, Rehovot, Israel and Max-Planck-Research-Unit for Ribosomal Structure, c/o DESY, Nötkestraße 85, W-2000 Hamburg, FRG

Nucleic Acids and Molecular Biology, Vol. 6
ed. by F. Eckstein and D.M.J. Lilley

2 Approximating the Shapes of the Ribosomal Particle at the Electron Microscopy Level

2.1 Image Reconstruction of Periodically Packed Ribosomes

Natural periodic organization of helices or ordered two-dimensional arrays of ribosomes had been observed in sections of eukaryotic cells exposed to stressful conditions, such as suboptimal temperatures, wrong diet or lack of oxygen. Some of these periodic forms were suitable for limited three-dimensional image reconstruction studies at low resolution. Despite the limited internal order of these systems and the inherent shortcomings of image reconstructions from thin sections of embedded crystals, namely the uncertainties regarding the exact sectioning directions and the chemical nature of the distribution of the stain within the particles, these studies yielded useful hints about the interactions between the particles, the outer contour of the ribosomes and the inner distribution of the ribosomal components (Kress et al. 1971; Lake and Slayter 1972; Unwin and Taddei 1977; Unwin 1979; O'Brien et al. 1980; Kühlbrandt and Unwin 1982; Milligan and Unwin 1982, 1986).

Similar reconstruction procedures were employed to analyze the three-dimensional microcrystals initially obtained from prokaryotic ribosomal particles (see below, Sect. 2.2). These were too small for X-ray crystallography but too thick for direct investigation by electron microscopy. Positively stained thin sections of four crystal forms of 50S subunits from *Bacillus stearothermophilus* (forms 1–4 in Yonath and Wittmann 1989a), with optical diffraction to 45–80 Å resolution, were used. These gave rise to four reconstructed models, all of a similar shape, consisting of two domains of unevenly distributed stain density (Fig. 1; Leonard et al. 1982; Yonath et al. 1986a). Ribosomal RNA is the most likely candidate for chemical interaction with uranyl acetate, the positive stain used for these reconstruction. Since there are numerous indications that the ribosomal RNA is distributed throughout the ribosome (for review, see Hardesty and Kramer 1986; Hill et al. 1990a), the models so obtained provide a crude approximation for the shape of the entire 50S subunit. It is noteworthy that the gross shapes of these models resemble the images of the 50S subunit which were reconstructed a few years later at a significantly higher resolution (28 Å), from negatively stained two-dimensional arrays grown under different conditions and exposed to a different experimental treatment (Fig. 1; Yonath et al. 1987a).

Ordered monolayers (also called two-dimensional arrays) are more suitable for three-dimensional image reconstruction, since they do not suffer from most of the shortcomings described above. The initially obtained two-dimensional arrays of ribosomal subunits from *E. coli* and *B. stearothermophilus* (Lake 1979; Arad et al. 1984) were grown within a few weeks from solution containing alcohols, and yielded diffraction quality

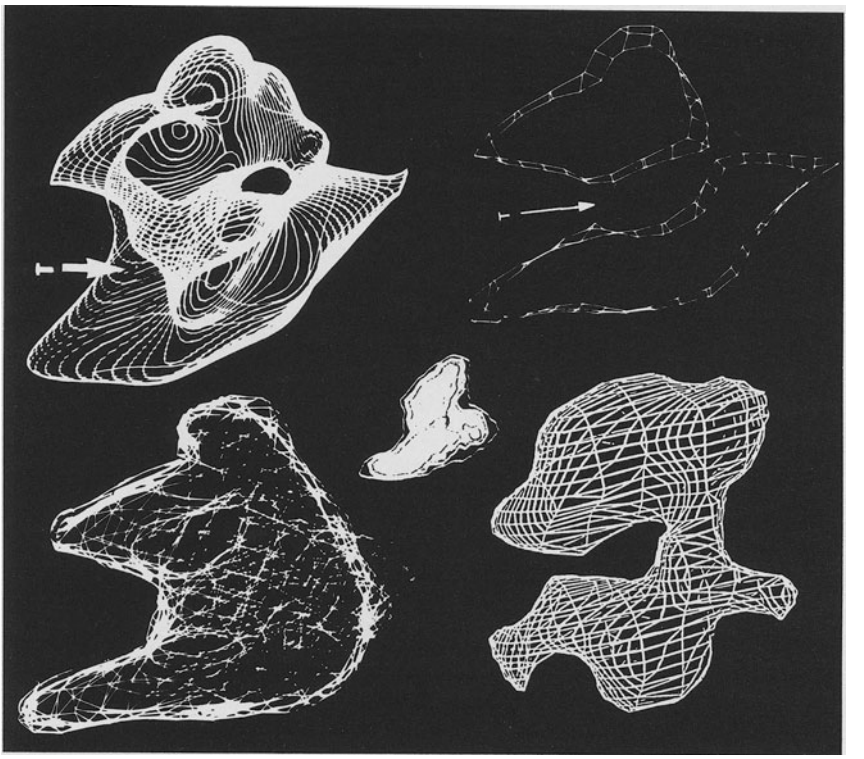

Fig. 1. Reconstructed images of 50S ribosomal subunit from *B. stearothermophilus*, obtained at 28 Å resolution from tilt series of negatively stained (with goldthioglucose) two-dimensional arrays (except *bottom left*). *T* shows the entrance to the tunnel. *Top right* The model of the 50S subunit, displayed in fine lines, showing clearly the entrance and exit of the tunnel. *Top left* A hand-drawn line was added, showing the border of the 50S subunit in an orientation similar to single 50S particles visualized by electron microscopy (the "crown view", Wittmann 1983). *Bottom right* A slice of 20Å thickness of the reconstructed model shown in the *top panel*. *Bottom left* The reconstructed stain density (at about 60 Å resolution) from positively stained thin sections of three-dimensional microcrystals of 50S subunits from *B. stearothermophilus*. *Middle insert* Filtered image of unstained sheets, viewed at cryotemperature. Note the similarities between the reconstructed image from the negatively stained two-dimensional sheets, the filtered image of the unstained array and the model reconstructed from the positively stained section, showing the stain distribution

marginally suitable for image reconstruction (Clark et al. 1982; Arad et al. 1984; Oakes et al. 1986a). The second generation two-dimensional arrays, of a much higher quality, were obtained within a few seconds, using combinations of salts and alcohols as crystallizing agents. Tilt series of arrays of 50S subunits and 70S ribosomes, negatively stained with an inert material, gold thioglucose, were suitable for image reconstructions (Figs. 1 and 2; Arad et al. 1987a,b; Yonath et al. 1987a).

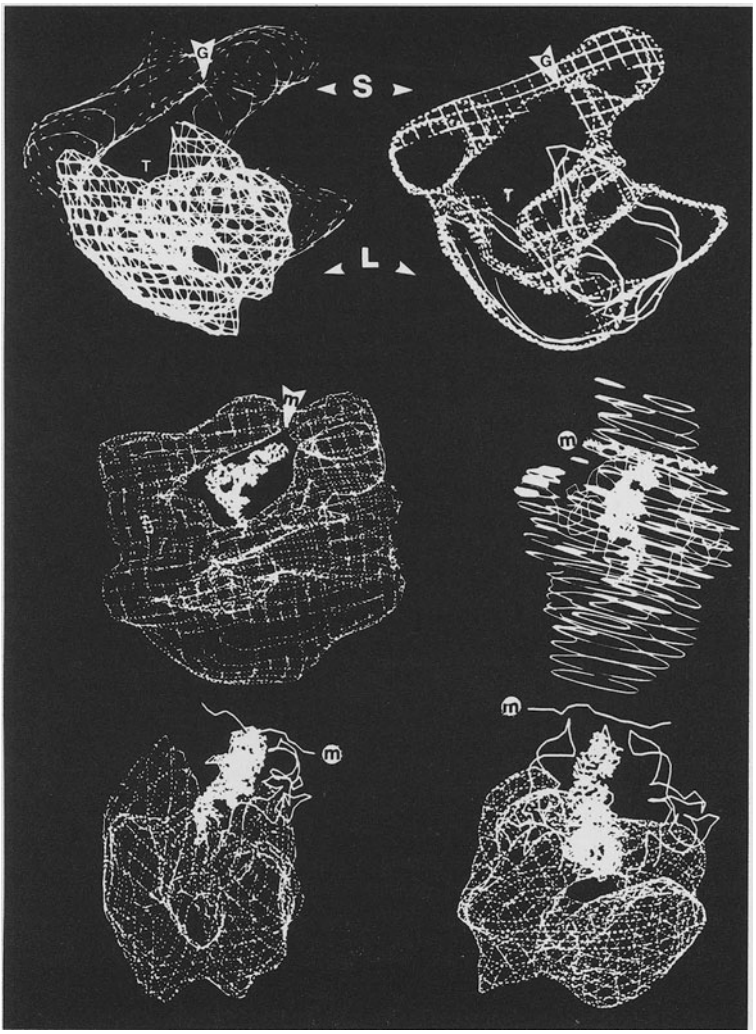

Fig. 2. Computer graphic displays of reconstructed models from tilt series of negatively stained (with goldthioglucose) two-dimensional arrays, viewed by electron microcopy, of 70S ribosome and its large subunit from *B. stearothermophilus*, into which mRNA and tRNA molecules were "model-built". *S* and *L* mark the small and the large subunits, respectively. *T* shows the entrance to the tunnel, *G* marks the groove in the small subunit, presumed to be the path of the mRNA (*m*). *Top panel* Superpositions of computer graphic displays of the outline of the reconstructed models of 70S (at 47 Å resolution) and the 50S ribosomal subunits (at 28 Å resolution). *Top left* Superposition of the model of the 50S subunit (shown as a *net*) on its corresponding location in the 70S ribosome (shown in *lines*). *Top right* A slice of the displayed models on the *left*, 50 Å in depth, in which the tunnel is *highlighted*. The 70S ribosome is shown as a *net*, the 50S subunit, in *lines*. *Middle panel* Two orthogonal views of the outline of the reconstructed model of the 70S ribosome. The envelope of the 70S particle is shown as a *dotted net* (*left*) and as *parallel lines* (*right*). Model built into the intersubunit free space: *m* is a segment of 28 ribonucleotides, in an arbitrary conformation, which may simulate the mRNA chain (highlighted by *arrowheads* on the *left*), togethr with three molecules of tRNA, two of which are shown as traces of their backbone, and the third one, which points directly into the tunnel is highlighted by including all its atoms. For clarity, only the highlighted tRNA molecule is shown on the *left*. *Bottom panel* The 50S subunit together with the model-built mRNA and tRNA (two molecules on the *left*, three on the *right*). The outline of the whole ribosome was removed for clarity

Structural information of a much higher detail is essential for an accurate determination of the shapes, the sizes and the detailed structures of the ribosomal particles. However, despite their relatively low resolution (47 and 28 Å, for the 70S and the 50S respectively), several key features, most of them associated with internal vacant spaces or partially filled hollows, which had not been detected earlier in prokaryotic ribosomes, were observed in the current reconstructed images from the two-dimensional arrays. The significant similarities in specific features of corresponding regions in the reconstructed models of the 50S and 70S particles were used to assess the reliability of the models, to locate the 50S subunit within the 70S ribosome, to suggest a model for associated 30S subunit and to tentatively assign biological functions to some structural features (Yonath and Wittmann 1989a; Berkovitch-Yellin et al. 1990; Yonath et al. 1990).

2.2 Tentative Assignments in the Reconstructed Models

2.2.1 A Plausible Path for Nascent Proteins

A tunnel of about 100 Å in length and up to 25 Å in diameter was detected in the reconstructed models of the 50S subunit and of the 70S ribosome, regardless of the staining procedure (Fig. 1; Yonath et al. 1987a, 1990; Yonath and Wittmann 1989a; Berkovitch-Yellin et al. 1990). A similar feature was seen in reconstructed images from two-dimensional arrays of eukaryotic ribosomes (Milligan and Unwin 1986) and in maps constructed from neutron diffraction data of crystals of 50S subunits of *Haloarcula marismortui* (Eisenstein et al. 1991). However, sophisticated three-dimensional image analysis of single 50S subunits of *E. coli* showed only an interface canyon alongside several holes and indentations (Frank et al. 1990).

Biochemical evidence, obtained first in the 1960s and reconfirmed recently, indicated that ribosomes mask the latest synthesized 25–40 amino acids of newly formed protein chains (Malkin and Rich 1967; Blobel and Sabatini 1970; Smith et al. 1978; Kurzchalia et al. 1988; Ryabova et al. 1988; Yen et al. 1988; Kolb et al. 1990). Complementing information was obtained by immunoelectron microscopy, showing that nascent proteins migrate out of the 50S subunit, in a site opposite to that of the biosynthetic reaction (Barnebeu and Lake 1982). Since the tunnel detected in the reconstructed images is of a width and a length suitable for the accommodation of growing polypeptide chains of 30–45 amino acids of any sequence at any conformation, this tunnel was suggested to be the path taken by the nascent protein.

In recent experiments, aimed at the verification of the existence of an internal tunnel, N-termini of nascent chains were detected by immuno-electron microscopy in two distinct patches on the 50S subunit: short poly-

peptides were found close to the subunit interface, and longer ones at the far end of this particle (Ryabova et al. 1988). It was also shown that ribosomes mask natural proteins more efficiently than artificial homopolymers (Kolb et al. 1990) and that homopolypeptides may choose an exit path slightly different from that of naturally occurring proteins (Hardesty et al. 1990). It is conceivable that a common feature located at the amino termini of natural proteins has a role in guiding the nascent protein chain into the tunnel. A failure in entering the tunnel may be fed back into the biosynthetic machinery at early stages, and may lead to the termination of the process. This hypothesis may explain why usually only 40–60% of well-prepared ribosomes are active in *in vitro* production of relatively long polypeptides, although almost all of the ribosomes bind mRNA and tRNA (Rheinberger and Nierhaus 1990) and why there are differences in the migration of short and long chains of newly synthesized polylysine or polyphenylalanine (Hardesty et al. 1990).

The chemical nature of the exit path is yet to be investigated. Preliminary mapping experiments showed that newly formed chains of polylysine and polyphenylalanine can be tightly attached to the large subunits of *E. coli* (Gilbert, 1963), *B. stearothermophilus* (Gewitz et al. 1988; Yonath et al. 1990) and *Haloarcula marismortuic* previousely named *Halobacteria marismortui*, Yonath et al. 1987b, 1990). Thus, it seems that the exit path of the nascent homopolypeptides is rich in rRNA and in hydrophobic regions, the components most likely to interact with polylysine and polyphenylalanine, respectively.

2.2.2 A Low-Resolution Model for Associated 30S and 50S Subunits

The approximate shape of the 30S subunit within the 70S ribosome was deduced by allocating the part of the 70S ribosome which visually corresponded best to that of the reconstructed 50S subunit and aligning the tunnel in the 70S ribosome with that found in the 50S subunit and (Fig. 2; Yonath and Wittmann, 1989a; Berkovitch-Yellin et al. 1990). The volumes and the overall shapes of the models of the 30S subunits derived in this way are rather similar to those proposed on the basis of investigations of individual 30S subunits (for reviews, see Wittmann 1983). The differences in the widths and lengths of the two models may reflect the conformational changes which occur upon the association of the two ribosomal subunits to form a 70S ribosome, or may originate from flattening of the isolated 30S particles on the electron microscope grid.

Although the overall agreement in the shapes of the reconstructed models of the 50S subunit and the corresponding part within the 70S ribosome is quite striking, there are two regions in which the two models differ slightly (Yonath and Wittmann 1989a; Berkovitch-Yellin et al. 1990; Yonath et al. 1990). At this stage it is not clear whether these differences

reflect conformational changes between free and bound subunits, or whether they result from differences in the resolutions of the two reconstructions.

2.2.3 The Intersubunit Space as the Site of Protein Biosynthesis

The small and large ribosomal subunits are well separated in almost all reconstructions of whole ribosomes, regardless of the reconstruction method, the source of the ribosomes or the level of organization: single particles (Wagenknecht et al. 1989; Frank et al. 1990), in situ sheets (Milligan and Unwin 1986) or in vitro two-dimensional arrays (Arad et al. 1987b; Yonath and Wittmann 1989a; Berkovitch-Yellin et al. 1990). The lower level of clarity of the separation between the subunits in some reconstructions may result from resolution limits as well as from shrinkage or collapse of the inspected ribosomes in the microscope vacuum (Wagenknecht et al. 1989).

The clearest separation was observed in the models reconstructed from two-dimensional arrays of 70S ribosomes from *B. stearothermophilus*. These contain an empty space at the subunit interface, comprising 15–20% of the volume within the envelope of the ribosome (Fig. 2). Spatial considerations showed that it is feasible that this intersubunit free space provides the location for the various enzymatic activities of protein biosynthesis. Thus, the intersubunit space is spacious enough to accommodate a relatively long segment of mRNA chain, up to three tRNA molecules and other non-ribosomal components which participate in protein biosynthesis. It is noteworthy that the intersubunit space may accommodate the tRNA molecules at various relative orientations, ranging from parallel, the lowest space-requiring arrangement, to perpendicular (Fig. 2), the highest space-consuming one (Spirin 1987).

As mentioned above, functional studies, carried out since the early days of ribosomology, showed that ribosomal RNA has an enzymatic role in the peptidyl transferase reaction. Specific affinity labelling proved instrumental in the elucidation of the role of the ribosomal RNA, and photosensitive agents were used to scan the environment of the peptidyl transferase center. These factors, together with the identification of conserved sequences of rRNA and model building experiments, identified several locations on the rRNA chains which are directly involved in key functional events (e.g. Zamir 1977; Moore 1988; Brimacombe et al. 1990; Cunnigham et al. 1990; Egebjerg et al. 1990; Ehreshman et al. 1990; Hill et al. 1990b; Noller et al. 1990; Oakes et al. 1990; Raue et al. 1990; Tappich et al. 1990).

Careful analysis of reconstructed images from non-stained arrays of eukaryotic ribosomes, investigated at cryogenic temperatures (Kühlbrandt and Unwin 1982; Milligan and Unwin 1986), as well as comparisons of reconstructed images obtained from in vitro grown two-dimensional arrays, stained with an inert material, with those stained by uranyl acetate, which may interact with the ribosomal RNA, showed a significant concentration of

rRNA at the subunit interface (Arad et al. 1987b; Yonath and Wittmann 1989a; Yonath et al. 1990). Another distinct region of crowded rRNA was revealed within the part of the 70S ribosome which was assigned as the bound 30S subunit (Fig. 2; Yonath and Wittmann 1989a; Berkovitch-Yellin et al. 1990; Yonath et al. 1990). Similarly, a region with of a high stain density was detected by electron microscope investigations of isolated 30S subunits (Oakes et al. 1990). In accord with biochemical and model-building experiments, which showed that the mRNA binds to the 30S subunits in an environment rich in rRNA (Brimacombe et al. 1988, 1990; Rinke-Apple et al. 1991), this region was tentatively identified as the approximate mRNA binding site.

A groove was clearly seen within the region of crowded rRNA on the 30S subunit. As during translation a segment of about 30–40 nucleotides of mRNA is masked by the ribosome (Kang and Cantor 1985), it is conceivable that the mRNA is progressing through this groove. The resolution of the reconstruction is too low for an accurate determination of the dimensions of the groove, but a rough estimation indicated that it may accommodate a stretch of the length of the masked segment at random, U-shaped or helical conformations.

tRNA is of a shape and size which allow its placement in the intersubunit space, so that its anticodon loop is associated with the mRNA, and its CCA terminus is positioned such that the newly formed peptidyl group may extend into the tunnel. In this orientation the tRNA molecule is able to form many non-cognate interactions with the walls of the intersubunit space (Fig. 2). At the current resolution of the reconstructions, both crystallographically determined orientations of tRNA, the native-closed and the bound-open one (for review, see Moras 1989), are indistinguishable.

3 Crystallographic Studies

3.1 RNA Molecules as Targets for Crystallographic Studies

A significant portion of the ribosomal RNA has been detected on the surface of the ribosome by chemical, biochemical and enzymatic experiments (see above, Sect. 2.2.3; also reviewed by Noller 1991), by direct probing with complimentary DNA (Hill et al. 1986, 1990b; Oakes et al. 1986b, 1990) and by contrasting or preferential staining of electron microscope samples (Leonard et al. 1982; Milligan and Unwin 1986).

Little is known about the molecular details of natural RNA macromolecules since the structures of very few RNA molecules and assemblies have been determined crystallographically thus far. In general, crystallization of RNA molecules and of assemblies containing RNA was found to be extremely difficult. In contrast to the stable periodic packing of DNA, RNA chains are loosely and irregularly packed. tRNA is the only family of RNA

molecules whose three-dimensional structure has been determined crystallographically, and even within this family, only a few members have been studied. Although the tRNA molecules are rather rigid, stable and of relatively low molecular weights (an average tRNA molecule is a chain of 76–90 nucleotides with a typical molecular weight of 25 kDa), many problems have been encountered in their crystallization and derivatization.

More serious problems were encountered in repeating efforts to determine the molecular structures of isolated ribosomal RNA. The growth of crystals, diffracting to 5–25 Å, of the lowest molecular weight ribosomal RNA, the 5S chain (of about 120 nucleotides), its fragment and its complex with a ribosomal protein (EL25), has been reported during the last decade (Morikawa et al. 1982; Abdul-Meguid et al. 1983; Lorenz et al. 1991), as of yet neither structure has been solved.

Among the large variety of natural complexes of RNA and proteins, the structures of only two types have been determined: RNA viruses and complexes of tRNA synthetases with their cognate tRNA molecules. An average virus is of a molecular weight similar to that of the ribosome (1–2 million daltons), but in contrast to ribosomes, viruses exhibit an exceptionally high internal symmetry which reduces the complexity of the crystallographic puzzle by 1–2 orders of magnitude. Most of the RNA viruses whose structures have been determined are very stable and their surfaces are composed mainly, or totally, of proteins with a natural tendency to pack periodically, thus they readily crystallize and their crystals are stable and well ordered (for review, see Jurnak and McPherson 1984). More severe problems have been encountered in the crystallization of the complexes containing tRNA and their synthetases. Only recently the molecular structures of the first two complexes have been determined crystallographically (Rould et al. 1989; Ruff et al. 1991; Rould and Steitz, this Vol.).

Being ribonucleoprotein complexes with no internal symmetry, notoriously flexible, unstable and routinely prepared as a population of mixed conformations, the suitability of ribosomes for structural studies has been doubtful. The existence of labile and readily hydrolyzed surface ribosomal RNA added substantial difficulties. On the other hand, the observations that cellular mechanisms can induce periodic packing of ribosomes (see Sect. 2.1) and the hypothesis that these ordered forms provide the physiological means for temporary storage of ribosomes stimulated attempts at their crystallization.

3.2 Halophilic and Thermophilic Ribosomal Particles Are Suitable for Crystallization

Bacterial ribosomes were chosen since they provide systems independent of in vivo events, environmental influences and physiological factors. For over a decade, extensive efforts were directed at the cystallization of *E. coli*

ribosomes. These attempts led to the growth of either two-dimensional arrays, marginally suitable for reconstitution studies (Lake 1979; Clark et al. 1982; Oakes et al. 1986a), or microcrystals, which could be investigated by electron microscopy but were too small for X-ray crystallography (Wittmann et al. 1982; Wittmann and Yonath 1985). More suitable sources for crystallizable ribosomes were halophilic and thermophilic bacteria (Table 1; Trackhanov et al. 1987, 1989; Yusupov et al. 1988). Presumably, the ribosomes from these organisms possess the required stability to retain their integrity during the long time needed for their isolation and crystallization.

The Dead Sea, which has the highest salt concentration of any natural body of water in the world, supports the growth of several species, among them the archaebacterium, *Haloarcula marismortui*. The ribosomes of this bacterium function under conditions which usually cause denaturation of proteins and dissociation of their assemblies with nucleic acids. Studies on the physicochemical properties of the halophilic ribosomes showed that they require more than 3 M salts for their activity, but maintain their integrity at significantly lower salt concentrations (Shevack et al. 1985). Consequently, a procedure has been developed for crystallization in solutions of the lowest concentrations of salts essential to avoid the disintegration of the ribosomes, and for collecting crystallographic data under conditions similar to the

Table 1. Characterized three-dimensional crystals of ribosomal particles

Source[a]	Grown form	Cell dimensions (Å)	Resolution (Å)[b]
70S T.t.	MPD[c]	524 × 524 × 306; $P4_12_12$	app. 20
70S T.t. + m-RNA and t-RNA[d]	MPD	524 × 524 × 306; $P4_12_12$	app. 15
30S T.t.	MPD	407 × 407 × 170; $P42_12$	7.3
50S H.m.	PEG[c]	210 × 300 × 581; $C222_1$	3.0
50S T.t.	AS[c]	495 × 495 × 196; $P4_12_12$	8.7
50S B.st.[e]	A[c]	360 × 680 × 920; $P2_12_12$	app. 18
50S B.st.[f]	PEG	308 × 562 × 395; 114°; C2	app. 11

[a] B.st = *Bacillus stearothermophilus*; T.t. = Thermus thermophilus; H.m. = Haloarcula marismortui.

[b] The highest resolution for which sharp diffraction spots could be consistently observed. In many instances we could not collect useful crystallographic data to this resolution.

[c] MPD, PEG, A, AS = crystals were grown by vapour diffusion in hanging drops from solutions containing methyl-pentane-diol (MPD), polyethyleneglycol (PEG), ammonium sulphate (AS) or low molecular weight alcohols (A).

[d] A complex including 70S ribosomes, 1.5–2 equivalents of $PhetRNA^{Phe}$ and an oligomer of 35 ± 5 uridines, serving as mRNA.

[e] Same form and parameters for crystals of large ribosomal subunits of a mutant (lacking protein BL11) from the same source and for modified particles with an undecagold cluster.

[f] Same form and parameters for crystals of a complex of 50S subunits, one tRNA molecule and a segment (18–20 mers) of a nascent polypeptide chain.

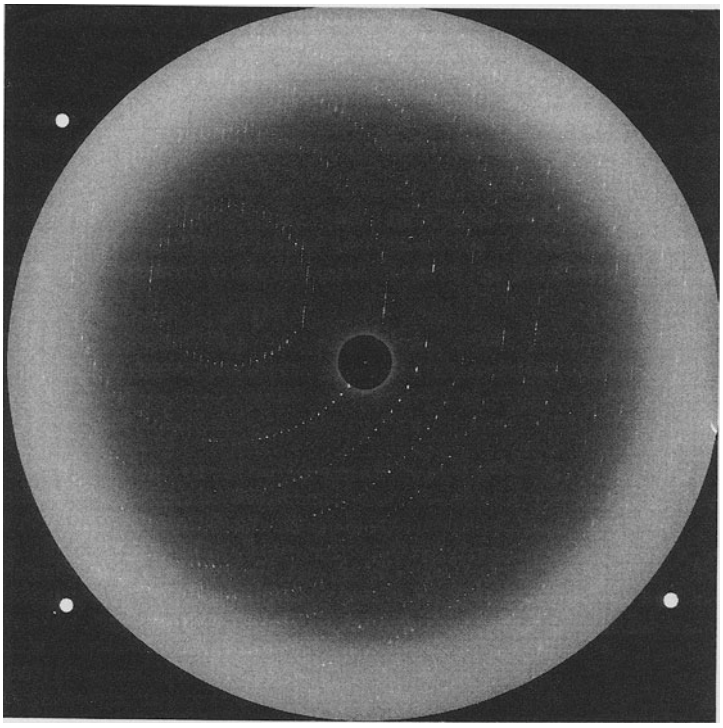

Fig. 3. 1.5° rotation pattern from a crystal of 50S ribosomal subunits from *Haloarcula marismortui*, grown by vapour diffusion in Linbro dishes coupled with individual seeding at 19°C from 6–8μl of: 5 mg/ml 50S subunits, 1.2 M potassium chloride, 0.5 M ammonium chloride, 0.005 M magnesium chloride, 0.001 M cadmium chloride and 5–6% polyethyleneglycol (6000), at pH 5.6 equilibrated with 1 ml reservoir of 1.7 M KCl and all the other components of the drop. The crystal was kept in 3 M potassium chloride, 0.5 M ammonium chloride, 0.005 M magnesium chloride, 0.001 M cadmium chloride and 8% polyethyleneglycol (6000), at pH 5.6. Before cooling it was soaked for 15 min in a solution containing the above storage components and 18% ethyleneglycol. The pattern was obtained at 90 K at station A1/CHESS. Crystal to film distance: 220 mm, diameter of collimator: 0.1 mm, wavelength: 0.9091 Å

physiological environment within the cell of this bacterium (Yonath and Wittmann 1989b).

Six crystal forms of the 50S and one of the 30S subunits from this bacterium were grown (Makowski et al. 1987; Yonath et al. 1990; von Böhlen et al. 1991). One of them diffracts to the highest resolution obtained so far from crystals of ribosomal particles: 3 Å (Fig. 3 and Table 1). This relatively high internal order was reached after extensive refinement of the growth conditions, including mild variations in the delicate equilibrium between mono- and divalent ions, the development of sophisticated seeding procedures (Makowski et al. 1987; Yonath and Wittmann 1989b) and the

addition of minute amounts of Cd^{2+} to the crystallization mixtures (von Böhlen et al. 1991).

The first ribosomal particles to be crystallized were the 50S subunits from the moderate thermophile *B. stearothermophilus*. The initially obtained microcrystals were unsuitable for crystallographic studies, but played a crucial role in the progress of the crystallography of ribosomes, since diffraction patterns of samples containing a large number of microcrystals, treated as "powder", contained features up to 3.5 Å resolution (Yonath et al. 1980) with spacing characteristic of ribosomal RNA (Klug et al. 1961; Langridge and Holmes 1962).

Seven crystal forms were obtained from these particles (Yonath and Wittmann 1989a; Yonath et al. 1990), two of them (Yonath et al. 1986b; Müssig et al. 1989) diffract to medium resolution (Table 1). It is of interest that the same crystallization conditions which yielded crystals from native particles were also suitable for the growth of crystals of mutated, reconstituted, complexed and derivatized subunits (Müssig et al. 1989; Weinstein et al. 1989).

The 70S ribosomes of the extreme thermophile *Thermus thermophilus* were crystallized in two similar forms (Trackhanov et al. 1989; Yonath et al. 1990). Crystals were also obtained from the two ribosomal subunits of this bacterium (Glotz et al. 1987; Yonath et al. 1988; Volkmann et al. 1990) as well as from subunits of a complex mimicking a defined stage in the biosynthetic process (see below; Hansen et al. 1990). Thus, this bacterium provides a system which may lead to the detection of gross conformational changes occurring upon subunit association and during the process of biosynthesis.

3.3 Some Common Properties of Ribosomal Crystals

Several common properties have been observed in the crystallization of prokaryotic ribosomal particles. In contrast to the short lifetime of isolated ribosomes, in all cases the crystallized ribosomes retain their integrity and biological activity for long periods, except for occasional mild fragmentation of the ribosomal RNA. Functional activity is a prerequisite for crystal growth, but not every active preparation yields high quality crystals. Thus, it seems that the requirements for crystallization are more severe than those needed for biological activity, and extreme care in growing the cells and in the preparation of the ribosomes is necessary for obtaining crystallizable particles. Furthermore, although the guidelines for successful crystallization were determined rather early (Yonath et al. 1982a), the exact conditions for the growth of quality crystals must be refined for each preparation. Thus the basic factors governing the quality of crystals relate more to the nature of the ribosomal particles than to the choice of the crystallizing agent (Yonath and Wittmann 1989b).

Specific problems in the crystallization of ribosomal particles may be attributed to the ribosomal RNA. As mentioned above, the ribosome's RNA is rather labile and can be easily fragmented. Some correlation between the integrity of the rRNA and the crystallizability of the ribosomal particles has been observed, indicating that higher quality crystals are obtained from ribosomes with minimum rRNA fragmentation, but does not rule out crystallization of ribosomal particles with somewhat nicked rRNA.

Mg^{2+} plays an essential role in maintaining the integrity of ribosomal particles. It was found that Mg^{2+} is also most crucial for the crystallization of ribosomal particles, presumably due to the participation of surface rRNA in the crystallographic net. In several cases an apparent competition was observed. For example, in spontaneous crystallization of 50S subunits, the lower the Mg^{2+} concentrations is, the thicker the crystals are. Interestingly, the upper critical value of Mg^{2+} permitted for the growth of three-dimensional crystals of 50S from *B. stearothermophilus* is the lowest needed for obtaining two-dimensional arrays (Arad et al. 1984).

Since ribosomes are large enough to be seen by electron microscopy, some steps in the nucleation and in the growth of their crystals could be followed. It was found that under proper crystallization conditions, the process of crystal growth starts within the first few hours by non-specific aggregation, which is likely to inhibit the natural tendency of ribosomes to disintegrate. At later stages these amorphous aggregates undergo rearrangements toward the formation of nuclei with various morphologies. Thus, nuclei which could lead to the formation of suitable crystals were found alongside lower order organizations such as star-shaped crystallites and various helical arrangements (Yonath et al. 1982b).

The formation of different morphologies within individual crystallization drops may be correlated with minute local differences in the composition of the drop. This may be the reason for the extreme sensitivity of the crystallization process to small changes in the crystallization conditions and may explain the rather high mosaic spread of ribosomal crystals. Therefore, it is not surprising that different crystal forms were developed under similar conditions, and that small variations in the growth media induce large differences in the crystallographic constants. An extreme example is the case of 70S ribosomes from *T. thermophilous*, for which the presence of 0.2 M KCl in the crystallization mixture caused a change of 65 Å in one unit cell axis, (Trackhanov et al. 1989; Yonath et al. 1990).

3.4 Crystalline Ribosomal Complexes

3.4.1 Complexes Containing 70S Ribosomes

All crystals of 70S particles obtained so far (from *E. coli*, *B. stearothermophilus* and *T. Thermophilus*) diffract to a very low resolution (20–

45 Å), which may be related to the inherent conformational heterogeneity of the ribosomal preparations. Artificial active ribosomes, constructed from purified 50S and 30S subunits which are expected to be fairly homogeneous, yielded crystals containing solely 50S subunits (Yonath et al. 1990; Berkovitch-Yellin et al. 1991), indicating that the interparticle interactions in the crystals of the 50S subunits are stronger than the affinity between the large and small subunits in 70S particles, kept for long periods without being activated in protein biosynthesis. These findings are in accord with observations made on two-dimensional arrays of 80S ribosomes, which could be depleted of the small subunits, but still maintained their packing integrity (Milligan and Unwin 1982), and highlight the readiness of the large ribosomal subunits to crystallize, a property which is also reflected in the large number of crystal forms obtained from bacterial 50S subunits (Yonath et al. 1980, 1986a–c, 1990; Yonath 1984; Makowski et al. 1987; Müssig et al. 1989; Volkmann et al. 1990; von Böhlen et al. 1991).

To minimize the flexibility and to increase the homogeneity of the crystallized material, complexes were prepared, containing ribosomes trapped in a conformation mimicking defined stages in protein biosynthesis. A primitive complex, composed of 70S ribosome from *T. thermophilus* with two phetRNA^{phe} molecules and a chain of about 35 uridyl residues, was crystallized. In this complex the mRNA is of a length which may fit into its groove in the 30S subunit (see Sect. 2.2.3) so that no long stretches of it project into the solvent, the intersubunit space is rather occupied and, above all, almost 90% of the ribosomes are in a similar conformation. Despite the non-optimal composition of this complex (e.g. a homopolynucleotide rather than an RNA chain of a designed sequence was used as mRNA), dramatic improvements in the reproducibility in crystal growth and in the internal order of the crystals were observed. Whereas the best crystals of 70S ribosomes (of *T. thermophilus*) diffract to 20–24 Å resolution (Trackhanov et al. 1989; Berkovitch-Yellin et al. 1991), the crystals of this complex exhibit sharp diffraction patterns to higher than 15 Å (Table 1; Hansen et al. 1990). To assess the individual contributions of the different components to the stability of this complex, 70S ribosomes were cocrystallized together with a chain of 35 uridines. Only poorly shaped crystals were occasionally grown, indicating the larger contribution of the tRNA to the stability of the complex.

3.4.2 Complexes of Ribosomal Subunits

Studies aimed at investigating the chemical properties of the exit path of the nascent chains by identifying compounds that adhere to it led to the crystallization of a second type of complexes, composed of large ribosomal subunits, short nascent polypeptides and tRNA molecules. As expected, the time needed for the translation of a given length of mRNA depends on its

sequence (Evers and Gewitz 1989), and various polypeptides differ in their ability to adhere to the ribosome. Using poly(U) or poly(A) as messenger RNA, small crystals have been grown from 50S subunits of either *H. marismortui* or *B. stearothermophilus*, together with a short nascent polyphenylalanine or polylysine (8–18 amino acids in length) and one molecule of their cognate tRNA (Gewitz et al. 1988; Müssig et al. 1989). In addition, conditions were determined for stoichiometric binding of $tRNA^{phe}$ to several ribosomal particles (Weinstein et al. 1991).

Since tRNA is part of all these complexes, it is an obvious target for indirect attachment of heavy-atom clusters to ribosomal crystals. As most of the interactions of tRNA with the ribosome are well characterized biochemically, crystallographic determination of the locations of the heavy-atom clusters attached to it should provide information, useful not only for phase determination but also for the localization of its binding site on the ribosome (see Sect. 4.1.2).

3.5 X-Ray and Neutron Crystallographic Data

Due to the weak diffracting power and the large unit cells of the crystalline ribosomal particles, virtually all X-ray crystallographic studies have to be performed with synchrotron radiation. This extremely intense, coherent and focussed X-ray beam is generated as a by-product of accelerators originally designed for high-energy particle experiments.

At ambient temperatures all ribosomal crystals decay at the first instance of X-radiation. The damage is so severe and rapid that the reflections beyond Bragg spacings of 15–18 Å, which are usually very weak, decay before they are irradiated for durations long enough to be detected. This extreme sensitivity led to the underestimation of the real resolution, to erroneous assignments of the cell parameters and to numerous difficulties in data collection and evaluation (Hope et al. 1989). It is assumed that the radiation damage is caused mainly by free radicals which are produced by the X-ray beam and propagate throughout the crystals. Therefore, a procedure was developed aimed at minimizing the freedom of movement of the free radicals by shock freezing the crystals and collecting their crystallographic data at cryogenic temperatures. Indeed, once appropriate conditions for shock-freezing had been established, crystals could be irradiated for days or weeks, and no measurable radiation damage was detected over time periods sufficient for collecting complete diffraction data sets from individual crystals. Furthermore, due to the possibility of long exposure even the higher resolution reflections, which are usually the weakest ones, could be detected.

Neutrons, in contrast to X-rays, cause essentially no damage in irradiated crystals at any temperature. Therefore, it is possible to conduct long measurements, required due to the weak diffraction of neutrons. Data to 30 Å

resolution were collected from crystals of 50S subunits from *H. marismortui* and phase sets were generated using direct methods. The resulting map contained compact regions with a shape similar to the reconstructed images of the large subunit from *B. stearothermophilus* (Eisenstein et al. 1991).

4 Phasing Algorithms

Crystallographic determination of the detailed three-dimensional structures of molecules is based on Fourier summation of all reflections, diffracted from the crystal upon irradiation. Each reflection is characterized by its direction, intensity and phase. The directions and amplitudes can be measured, whereas the phases have to be determined indirectly.

4.1 Derivatization with Multiple Heavy Atom Clusters

The most commonly used method for phasing in biological crystallography is multiple isomorphous replacement (MIR). This method is based on the introduction of electron-dense atoms to the crystalline lattice at one or a few distinct locations. The added atoms have to be dense enough to cause measurable changes in the diffraction pattern while keeping the crystal isomorphous with that of the native molecule. Due to the enormous size of the ribosome and the lack of internal symmetry, compact clusters of a large number of heavy atoms, linked directly to each other, should be appropriate for derivatization.

Suitable derivatives of biological macromolecules are usually obtained by soaking crystals in solutions of the heavy-atom compound or by co-crystallization of the macromolecule together with the heavy atom. For ribosomes, with their enormous and complex surface area, the chances are slim for obtaining a single binding site with full occupancy by soaking. Therefore, an alternative procedure has been developed, based on covalent binding of the heavy atom at a specific site on the ribosome before crystallization. This approach requires sophisticated synthetic techniques and time-consuming purification procedures, but at the same time it should lead to suitable derivatives.

4.1.1 Binding of Dense Clusters to Ribosomal Particles

Monofunctional reagents have been prepared from undecagold (Jahn 1989a) and tetrairidium (Jahn 1989b) clusters. The accessibility of the bulky gold cluster was enhanced by attaching a maleimido group at the far end of chains of differing lengths. Conditions were defined to minimize the number of exposed sulfhydryl groups which can bind the gold cluster (at different

yields) to one to three sulfhydryls on the surface of each ribosomal particle which has been studied by us so far (2). In this way single sites on 70S ribosomes and on 30S subunits from *T. thermophilus* were almost quantitatively derivatized (Weinstein et al. 1991) and crystals smaller than, but isomorphous with, the native ones were grown from the modified particles. A lower yield was obtained for the binding of the gold cluster of the 50S subunit from *B. stearothermophilus* and *H. marismortui.*

Since direct binding of the clusters to the surfaces of intact ribosomal particles cannot be fully controlled, a more effective procedure was developed, based on the ability to partially or fully reconstitute active ribosomes from their isolated components. An example is the derivatization of the 50S ribosomal subunits from *B. stearothermophilus*. Ribosomes of a mutant of this bacterium which lacks protein BL11 (Schnier et al. 1990) were used. Since mutated 70S ribosomes and 50S subunits were crystallized isomorphously with those of the respective wild-type particles (Yonath et al. 1986c, 1990; Müssig et al. 1989), it was deduced that the absence of protein BL11 did not cause gross conformational changes in the ribosome or destroy the crystallographic network. These single-site derivatized 50S ribosomal subunits were crystallized and led to reasonable diffraction data.

In similar experiments several proteins were quantitatively removed from the ribosomes of *H. marismortui*. These could be fully reconstituted into core particles. One of the detached proteins, HL11, binds reagents specific to -SH groups, but, in contrast to BL11, the modified protein could not be incorporated into the core particle. Consequently, the original purpose, derivatization of the halophilic 50S subunits, was not achieved, but this experiment provided a tool for isolation of protein HL11 and for obtaining core particles, lacking HL11, similar to the mutated ribosomes from *B. stearothermophilus*. For the case of *H. marismortui*, which is extremely resistant to antibiotics, such procedures may replace mutagenesis. Crystals of the depleted core were obtained (von Böhlen et al. 1991). These may be useful for locating the site of HL11 in the ribosome. Incorporation of natural or engineered -SH groups into the surface of the ribosome is an extension of these procedures. The rather advanced stages of the genetic sequencing of the halophilic ribosomal proteins (Bergmann and Arndt 1990), the possibility to incorporate selected non-self ribosomal proteins into depleted halophilic ribosomal cores (Koepke et al. 1990), the ability to isolate in situ halophilic ribonucleic-protein complexes (U. Evers, pers. comm.) and the determination of conditions for reconstitution of halophilic ribosomes (Sanchez et al. 1990) are being exploited with this aim.

4.1.2 Labelling Natural Carriers by Heavy Atom Cluster

As mentioned in Section 3.3, conditions for stoichiometric binding of tRNA to several ribosomal particles have been determined and two types of com-

plexes containing tRNA were crystallized. Base 47 of *E. coli* $tRNA^{phe}$ is a naturally modified uridine nucleoside (ACP3U), containing an exposed reactive primary amino group. Iminothiolane was used to convert this amino group into a reactive sulfhydryl, which, in turn, was used to bind the gold cluster. Using radioactive $tRNA^{phe}$-GC (Boeckh and Wittmann 1991), it was observed that the modified molecule could be aminoacylated by its synthetase with the same rates and yields as the native molecule. In addition, $tRNA^{phe}$-GC binds to 30S ribosomal subunits from *Thermus thermophilus* with the same stoichiometry as found for native $tRNA^{phe}$, in the presence and absence of poly(U) (Weinstein et al. 1991).

In principle any compound that forms a tight and specific complex with ribosomal particles can be used as a carrier for the heavy-atom clusters. Since the interactions of such carriers with the ribosomes are or can be well characterized, the crystallographic determination of their sites should provide information, useful not only for phase determination but also for the localization of their binding sites on the ribosome.

4.2 Other Phasing Methods

Attempts at phasing have also been made, assuming that at low resolution the gross structural features of bacterial ribosomes are sufficiently similar. The approximated reconstructed models (Sect. 2.1) of the 70S ribosome and the 50S ribosomal subunit (from *B. stearothermophilus*) have been exploited together with crystallographic data obtained from crystals of ribosomal particles from *Th. thermophilus* and *H. marismortui*, for real and reciprocal space searches (D. Rabinovich, M. Eisenstein, Z. Berkovitch-Yellin, R. Sharon and A. Yonath, unpubl. data). Parallel attempts, exploiting direct methods for phasing have also yielded encouraging results (S. Subbiah, M. Roth, E. Pebay-Peroula, N. Volkmann, F. Schlünzen, M. Eisenstein, Z. Berkovitch-Yellin, W. Bennett and A. Yonath, unpubl. data).

5 Concluding Remarks

This chapter attempts to demonstrate the achievements and the obstacles in structural studies of a large and flexible natural ribonucleoprotein complex, the ribosome. Of particular interest are the findings that crystals, diffracting to almost atomic resolution, could be obtained from these giant assemblies; that it is possible to quantitatively label ribosomal particles and ribosomal components as well as individual tRNA molecules by large heavy-atom clusters without impairing their integrity and biological activity; that crystals of ribosomes, trapped in different functional states together with non-ribosomal components, paricipating in protein biosynthesis, can be analyzed crystallographically; and that features not seen earlier in prokaryotic ribo-

somes could be observed in image reconstructions of two-dimensional sheets.

Acknowledgements. The studies presented here have been carried out under the inspiration and guidance of the late Prof. H.G. Wittmann. Experiments were performed at the Max Planck Research Unit in Hamburg, the Max Planck Institute for Molecular Genetics in Berlin and the Weizmann Institute of Science, Israel. The following facilities were used: the EMBL Laboratory in Heidelberg (for image reconstruction), the ILL neutron diffraction facility in Grenoble; and the following synchrotron facilities: EMBL/DESY, Hamburg; CHESS/Cornell University; SSRL, Stanford University; SRS/Daresbury, UK; and KEK/PF, Japan.

Support was provided by the National Institutes of Health (NIH GM 34360), the Federal Ministry for Research and Technology (BMFT 05 180 MP BO), the USA-Israel Binational Foundation (BSF 85-00381), the France-Israel Binational Foundation (NRCD-334190), the Kimmelman Center for Macromolecular Assembly at the Weizmann Institute, the Minerva and the Heinemann Foundations (4694 81). AY holds the Martin S. Kimmel professorial chair.

References

Abdul-Meguid SS, Moore PB, Steitz TA (1983) Crystallization of a ribonuclease-resistant fragment of *E. coli* 5S ribosomal RNA and its complex with protein 125. J Mol Biol 171:207–215

Arad T, Leonard KR, Wittmann HG, Yonath A (1984) Two-dimensional crystalline sheets of *B. stearothermophilus* ribosomal particles. EMBO J 3:127–131

Arad T, Piefke J, Gewitz HS, Hennemann B, Glotz C, Müssig J, Yonath A, Wittmann HG (1987a) The growth of ordered two-dimensional sheets of ribosomal particles from salt-alcohol mixtures. J Anal Biochem 167:113–117

Arad T, Piefke J, Weinstein S, Gewitz HS, Yonath A, Wittmann HG (1987b) Three-dimensional image reconstruction from ordered arrays of 70S ribosomes. Biochimie 69:1001–1005

Barnebeu C, Lake JA (1982) Nascent polypeptide chains emerge from the exit domain of the large ribosomal subunit: immune mapping of the nascent chain. Proc Natl Acad Sci USA 79:3111–3115

Bergman U, Arndt E (1990) Evidence for an additional archaebacterial gene cluster in *Halobacterium marismortui* encoding ribosomal proteins HL46e and HL30. Biochem Biophys Acta 1050:56–60

Berkovitch-Yellin Z, Wittmann HG, Yonath A (1990) Low resolution models for ribosomal particles reconstructed from electron micrographs of tilted two-dimensional sheets: tentative assignments of functional sites. Acta Crystallogr B46:637–643

Berkovitch-Yellin Z, Hansen H, Bennett WS, Sharon R, von Böhlen K, Volkmann N, Piefke J, Yonath A, Wittmann HG (1991a) Crystals of 70S ribosomes from thermophilic bacteria are suitable for X-ray analysis at low resolution, J Crystal Growth 110:208–213

Berkovitch-Yellin Z, Bennett WS, Yonath A (1991b) Aspects in structural studies on ribosomes. CRC Rev Bioch (in press)

Blobel G, Sabatini DD (1970) Controlled proteolysis of nascent polypeptides in rat liver cell fractions. J Cell Biol 45:130–145

Boeckh T, Wittmann HG (1991) Synthesis of a radioactive labeled undecagold cluster for application in X-ray structure analysis of ribosomes. Biochem Biophys Acta 1075:50–55

Brimacombe R, Amadja J, Stiege W, Schueler D (1988) A detailed model of the three-dimensional structure of *E. coli* 16S ribosomal RNA in situ in the 30S subunit. J Mol Biol 199:115–136

Brimacombe R, Greuer B, Mitcell P, Osswald M, Rinke-Appel J, Schueler, D. Stade K (1990) Three-dimensional structure and function of *E. coli* 16S and 23S rRNA as studied by cross-linking techniques. In: Hill EW, Dahlberg A, Garrett RA, Moore PB, Schlesinger D, Warner JR (eds) The ribosomes, structure, function and evolution. Am Soc Microbiol, Washington, pp 93–106

Clark W, Leonard KR, Lak J (1982) Ribosomal crystalline arrays of large subunits from *E. coli*. Science 216:999–1000

Cunnigham PR, Weizmann CJ, Nrgre D, Sinning JG, Frick V, Nurse K, Ofengand J (1990) In vitro analysis of the role of rRNA in protein biosynthesis: site specific mutation and methylation. In: Hill EW, Dahlberg A, Garrett RA, Moore PB, Schlesinger D, Warner JR (eds) The ribosomes, structure, function and evolution. Am Soc Microbiol, Washington, pp 243–252

Egebjerg J, Larsen N, Garrett RA (1990) Structural map of 23S rRNA. In: Hill EW, Dahlberg A, Garrett RA, Moore PB, Schlesinger D, Warner JR (eds) The ribosomes, structure, function and evolution. Am Soc Microbiol, Washington, pp 168–179

Ehreshmann B, Ehreshmann C, Romby P, Mougel M, Baudin F, Westhof E, Ebel JP (1990) Detailed structure of rRNA: new approaches. In: Hill EW, Dahlberg A, Garrett RA, Moore PB, Schlesinger D, Warner JR (eds) The ribosomes, structure, function and evolution. Am Soc Microbiol, Washington, pp 148–159

Eisenstein M, Sharon R, Berkovitch-Yellin Z, Gewitz HS, Weinstein S, Pebay-Peyroula E, Roth M, Yonath A (1991) The interplay between X-ray crystallography, neutron diffraction, image reconstruction, organo-metallic chemistry and biochemistry in structural studies of ribosomes. Biochemie 73:879–886

Evers U, Gewitz HS (1989) Studies on the accessibility of nascent non-helical peptide chains on the ribosomes. Biochem Int 19:1031–1038

Frank J, Verschoor A, Radamaacher M, Wagenknecht T (1990) Morphologies of eubacterial and eukaryotic ribosomes as determined by three dimensional electron microscopy. In: Hill EW, Dahlberg A, Garrett RA, Moore PB, Schlesinger D, Warner JR (eds) The ribosomes, structure, function and evolution. Am Soc Microbiol, Washington, pp 107–113

Gewitz HS, Glotz C, Piefke J, Yonath A, Wittmann HG (1988) Two-dimensional crystalline sheets of the large ribosomal subunits containing the nascent protein chain. Biochimie 70:645–648

Gilbert W (1963) Protein synthesis in *E. coli*. Cold Spring Harbor Symp Quant Biol 28:287–294

Glotz C, Müssig J, Gewitz HS, Makowski I, Arad T, Yonath A, Wittmann HG (1987) Three-dimensional crystals of ribosomes and their subunits from eu- and archaebacteria. Biochem Int 15:953–960

Hansen H, Volkmann N, Piefke J, Glotz C, Weinstein S, Makowski I, Meyer S, Wittmann HG, Yonath A (1990) Crystals of complexes mimicking protein biosynthesis are suitable for crystallographic studies. Biochim Biophys Acta 1050:1–8

Hardesty B, Kramer G (1986) Structure, function and genetics of ribosomes. Springer, Berlin Heidelberg New York

Hardesty B, Picking WD, Odom OW (1990) The extension of polyphenyl alanynine and polylysine peptides on *E. coli* ribosomes. Biochim Biophys Acta 1050:197–202

Hill WE, Trappich BE, Tassanakajohn B (1986) Probing ribosomal structure and function. In: Hardesty B, Kramer G (eds) Structure, function and genetics of ribosomes. Springer, Berlin Heidelberg New York, pp 233–256

Hill EW, Dahlberg A, Garrett RA, Moore PB, Schlesinger D, Warner JR (eds) (1990a) The ribosomes: structure, function and evolution. Am Soc Microbiol, Washington

Hill WE, Weller J, Gluick T, Merryman C, Marconi RT, Tassanakajohn A, Tappich WE (1990b) Probing ribosome structure and function by using short complementary DNA oligomers. In: Hill EW, Dahlberg A, Garrett RA, Moore PB, Schlesinger D, Warner JR (eds) The ribosomes, structure, function and evolution. Am Soc Microbiol, Washington, pp 253–264

Hope H, Frolow F, von Böhlen K, Makowski I, Kratky C, Halfon Y, Danz H, Webster P, Bartels K, Wittmann HG, Yonath A (1989) Cryocrystallography of ribosomal particles. Acta Crystallogr B45 (345):190–199

Jahn W (1989a) Synthesis of water soluble undecagold cluster for specific labeling of proteins. Z Naturforsch 44b:1313–1322

Jahn W (1989b) Synthesis of water soluble tetrairidium clusters suitable for heavy atom labeling of proteins. Z Naturforsch 44b:79–82

Jurnak FA, McPherson A (eds) (1984) Biological macromolecules and assemblies I. Virus structures. John Wiley & Sons, New York

Kang C, Cantor CR (1985) Structure of ribosome bound mRNA as revealed by enzymatic accessibility studies. J Mol Biol 210:659–663

Klug A, Holmes KC, Finch JT (1961) X-ray diffraction studies on ribosomes from different sources. J Mol Biol 3:87–100

Koepke AKE, Paulke C, Gewitz HS (1990) Overexpression of methanococcal ribosomal protein L12 in *E. coli* and its incorporation into halobacterial 50S subunits yielding active ribosomes, J Biol Chem 265:6436–64

Kolb VA, Kommer A, Spirin AS (1990) Nascent peptide and the ribosomal tunnel. Worksh translation, Leiden, p 84a

Kress Y, Wittner M, Rosenbaum RM (1971) Sites of cytoplasmic ribonucleoprotein-filament assembly in relation to helical body formation in axenic trophozoites of *Entamoeba histolytica*. J Cell Biol 49:773–784

Kühlbrandt W, Unwin PNT (1982) Distribution of RNA and proteins in crystalline eukaryotic ribosomes. J Mol Biol 156:431–488

Kurzchalia SV, Wiedmann M, Breter H, Zimmermann W, Bauschke E, Rapoport TA (1988) tRNA-mediated labeling of proteins with biotin, a nonradioactive method for the detection of cell-free translation products. Eur J Biochem 172:663–668

Lake JA (1979) Ribosome structural ad functional sites. In: Chambliss G, Craven GR, Davies J, Davis K, kahan L, Nomura M (eds) Ribosomes structure, function and genetics. University Park Press, Baltimore, pp 207–236

Lake JA, Slayter H (1972) Three-dimensional structure of the chromatoid body helix of entamoeba invades. J Mol Biol 66:271–282

Langridge R, Holmes KC (1962) X-ray diffraction studies of concentrated gels of ribosomes from *E. coli*. J Mol Biol 5:611–618

Leonard KR, Arad T, Tesche B, Erdmann VA, Wittmann HG, Yonath A (1982) Crystallization, electron microscopy and three-dimensional reconstruction studies of ribosomal subunits. In: Le Poole JB, Zeitler E, Thomas G, Schimmel G, Weichman C, Bassewitz KV (eds) Electron microscopy 1982, vol 3. Hartung, Hamburg, pp 9–15

Lorenz S, Betzel C, Raderschall E, Dauter Z, Wilson KS, Erdmann VA (1991) Crystallization and preliminary diffraction studies of 5S RNA from the thermophilic bacterium *Thermus flavus*. J Mol Biol 219:390–402

Makowski I, Frolow F, Saper MA, Wittmann HG, Yonath A (1987) Single crystals of large ribosomal particles from *Halobacterium marismortui* diffract to 6 Å. J Mol Biol 193:819–821

Malkin LI, Rich A (1967) Partial resistance of nascent polypeptide chains to proteolytic digestion due to ribosomal shielding. J Mol Biol 26:329–346

Milligan RA, Unwin PNT (1982) In vitro crystallization of ribosomes from chick embryos. J Cell Biol 95:648–652

Milligan RA, Unwin PNT (1986) Location of the exit channel for nascent proteins in 80S ribosomes. Nature (London) 319:693–696

Moore P (1988) The ribosome returns. Nature (London) 331:223–229

Moras D (1989) Crystal structure of tRNAs. In: Saenger W (ed) Landolt-Börnstein, new ser 1b. Nucleic acids. Springer, Berlin Heidelberg New York, pp 1–30

Morikawa K, Kawakami M, Takenura S (1982) Crystallization and Preliminary diffraction studies of 5S RNA from *Thermus thermophilus* HB8. FEBS Lett 145:194–196

Müssig J, Makowski I, von Böhlen K, Hansen H, Bartels KS, Wittmann HG, Yonath A (1989) Crystals of wild-type, mutated, derivatized and complexed 50S ribosomal

subunits from *Bacillus stearothermophilus* suitable for X-ray analysis. J Mol Biol 205:619–621
Noller HF (1991) Ribosomal RNA and translation. Annu Rev Biochem 60:191–227
Noller HF, Moazed D, Stern S, Powers T, Allen PN, Robertson BW, Triman K (1990) In: Hill EW, Dahlberg A, Garrett RA, Moore PB, Schlesinger D, Warner JR (eds) The ribosomes, structure, function and evolution. Am Soc Microbiol, Washington, pp 73–92
Oakes M, Henderson E, Scheiman A, Clark M, Lake J (1986a) Ribosome structure, function and evolution: mapping ribosomal RNA, proteins and functional site in three dimensions. In: Hardesty B, Kramer G (eds) Structure, function and genetics of ribosomes. Springer, Berlin Heidelberg New York, pp 47–67
Oakes M, Clarck M, Henderson E, Lake J (1986b) DNA hybridization electron microscopy: ribosomal RNA nucleotides 1392–1407 are exposed in the cleft of the small subunit. Proc Natl Acad Sci USA 83:275–918
Oakes M, Scheiman A, Atha T, Shakweiler G, Lake J (1990) Ribosome structure: three-dimensional location of rRNA and proteins. In: Hill EW, Dahlberg A, Garrett RA, Moore PB, Schlesinger D, Warner JR (eds) The ribosomes, structure, function and evolution. Am Soc Microbiol, Washington, pp 180–193
O'Brien L, Shelley K, Towfighi J, McPherson A (1980) Crystalline ribosomes are present in brain of senile humans. Proc Natl Acad Sci USA 77:2260–2264
Raue HA, Munster W, Rutgers CA, Riet JV, Planta R (1990) rRNA: from structure to function. In: Hill EW, Dahlberg A, Garrett RA, Moore PB, Schlesinger D, Warner JR (eds) The ribosomes, structure, function and evolution. Am Soc Microbiol, Washington, pp 217–235
Rheinberger HJ, Nierhaus KH (1990) Partial release of AcPhe2-tRNA from ribosome during poly(U) dependent poly(phe) synthesis and the effects of chloramphenicol. Eur J Biochem 193:643–650
Rinke-Apple J, Jünke N, Stade K, Brimacombe R (1991) The path of mRNA through *E. coli* ribosome, site directed cross-linking of mRNA analogues carrying a photo-reactive label at various points 3′ to the decoding site. EMBO J 10:2195–2202
Rould MA, Perona JJ, Soell D, Steitz TA (1989) Structure of *E. coli* glutamyl-tRNA synthetase complexed with $tRNA^{glu}$ and ATP at 2.8 Å resolution: implications for tRNA discrimination Science 246:1135–1142
Rould MA, Steitz TA (1992) Structure of the synthetase-tRNA glu-ATP complex. In: Eckstein F, Hilley, DM (eds) Biology, Vol. 6, Springer, Berlin Heidelberg pp
Ruff M, Krishnaswamy S, Boeglin M, Poterszman A, Mitchler A, Podjarny A, Moras D (1991) Class II aminoacyl tRNA synthetases: crystal structure of yeast aspartyl-tRNA synthetase complexed with $tRNA^{asp}$. Science 252:1682–1689
Ryabova LA, Selivanova OM, Baranov VI, Vasiliev VD, Spirin AS (1988) Does the channel for nascent peptide exist inside the ribosome? FEBS Lett 226:255–260
Sanchez ME, Urena D, Amils R, Londei P (1990) In vitro reassembly of active large ribosomal subunits of the halophilic archaebacterium *Halogax mediterrane*, Biochemistry 29:9256–9259
Schnier J, Gewitz HS, Behrens E, Lee A, Ginther G, Leighton T (1990) Isolation and characterization of *Bacillus stearothermophilus* 30S and 50S ribosomal protein mutations. J Bacteriol 172:7306–7309
Shevack A, Gewitz HS, Hennemann B, Yonath A, Wittmann HG (1985) Characterization and crystallization of ribosomal particles from *Halobacterium marismotoui*. FEBS Lett 184:68–71
Smith WP, Tai PC, Davis BD (1978) Interaction of secreted nascent chains with surrounding membranes in *Bacillus subtilis*. Proc Natl Acad Sci USA 75:5922–5925
Spirin A (1987) Structural dynamic aspects of protein synthesis on ribosomes. FEBS Lett 69:949–956
Tappich WE, Goerringer HU, De Stasio E, Prescott C, Dahlenberg AE (1990) Studies on ribosome function by mutagenesis of *E. coli* rRNA In: Hill EW, Dahlberg A, Garrett RA, Moore PB, Schlesinger D, Warner JR (eds) The ribosomes, structure, function and evolution. Am Soc Microbiol, Washington, pp 236–243

Trackhanov SD, Yusupov MM, Agalarov SC, Garber MB, Ryazantsev SN, Tischenko SV, Shirokov VA (1987) Crystallization of 70S ribosomes and 30S ribosomal subunits from *Thermus thermophilus*. FEBS Lett 220:319–322

Trackhanov SD, Yusupov MM, Shirokov VA, Garber MB, Mitschler A, Ruff M, Thierry JC, Moras D (1989) Preliminary X-ray investigation of 70S ribosome crystals from *Thermus thermophilus*. J Mol Biol 209:327–331

Unwin PNT (1979) Attachment of ribosome crystals to intracellular membranes. J Mol Biol 132:69–79

Unwin PNT, Taddei C (1977) Packing of ribosomes in crystals from the lizard *Lacerta sicula*. J Mol Biol 114:491–499

Volkmann N, Hottentrager S, Hansen H, Zayzsev-Bashan A, Sharon R, Berkovitch-Yellin Z, Yonath A, Wittmann HG (1990) Characterization and preliminary crystallographic studies on large ribosomal subunits from *Thermus thermophilus*. J Mol Biol 216:239–241

Von Böhlen K, Makowski I, Hansen HAS, Bartels H, Berkovitch-Yellin Z, Zaytzev-Bashan A, Meyer S, Paulke C, Franceschi F, Yonath A (1991) Single crystals of large ribosomal particles from *Halobacterium marismortui* diffract to 3 Å. J Mol Biol 222:11–15

Wagenknecht T, Graassucc R, Frank J (1989) Electron microscopy and computer image averaging of ice-embedded large ribosomal subunits from *E. coli*. J Mol Biol 199:137–147

Weinstein S, Jahn W, Hansen HAS, Wittmann HG, Yonath A (1989) Novel procedures of derivatization of ribosomes for crystallographic studies. J Biol Chem 264:19138–19142

Wittmann HG (1983) Architecture of prokaryotic ribosomes. Annu Rev Biochem 52:35–65

Wittmann HG, Yonath A (1985) Diffraction studies on crystals of ribosomal particles. In: Ts'o POP, Nicollini C (eds) The structure and function of genetic apparatus. Plenum, New York, pp 177–189

Wittmann HG, Müssig J, Gewitz HS, Piefke J, Rheinberger HJ, Yonath A (1982) Crystallization of *E. coli* ribosomes. FEBS Lett 146:217–220

Yen IJ, Macklin PS, Cleavland DW (1988) Autoregulated instability of beta-tubulin mRNAs by recognition of the nascent amino terminus of beta-tubulin. Nature (London) 334:580–585

Yonath A (1984) Three-dimensional crystals of ribosomal particles. TIBS 9:227–230

Yonath A, Wittmann HG (1988) Approaching the molecular structure of ribosomes. J Biophys Chem 29:17–29

Yonath A, Wittmann HG (1989a) Challenging the three-dimensional structure of ribosomes. TIBS 14:329–335

Yonath A, Wittmann HG (1989b) Crystallographic and image reconstruction studies on ribosomal particles from bacterial sources. Meth Enzymol 164:95–117

Yonath A, Müssig J, Tesche B, Lorenz S, Erdmann VA, Wittmann HG (1980) Crystallization of the large ribosomal subunit from *B. stearothermophilus*. Biochem Int 1:428–435

Yonath A, Müssig J, Wittmann HG (1982a) Parameters for crystal growth of ribosomal subunits. J Cell Biochem 19:145–155

Yonath A, Khavitch G, Tesche B, Müssig J, Lorenz S, Erdmann VA, Wittmann HG (1982b) The nucleation of crystals of the large ribosomal subunits from *B. stearothermophilus*. Biochem Int 5:629–639

Yonath A, Saper MA, Makowski I, Müssig J, Piefke J, Bartunik HD, Bartels KS, Wittmann HG (1986a) Characteriation of single crystals of the large ribosomal particles from *B. stearothermophilus*. J Mol Biol 187:633–636

Yonath A, Saper MA, Wittmann HG (1986b) Structural studies on ribosomal particles. In: Hardesty B, Kramer G (eds) Structure, function and genetics of ribosomes. Springer, Berlin Heidelberg New York, pp 112–129

Yonath A, Saper MA, Frolow F, Makowski I, Wittmann HG (1986c) Characterization of single crystals of large ribosomal particles from a mutant of *B. stearothermophilus*. J Mol Biol 192:161–162

Yonath A, Leonard KR, Wittman HG (1987a) A tunnel in the large ribosomal subunit revealed by three-dimensional image reconstruction. Science 236:813–816

Yonath A, Leonard KR, Weinstein S, Wittmann HG (1987b) Approaches to the determination of the three-dimensional architecture of ribosomal particles. Cold Spring Harbor Symp Quant Biol 52:729–741

Yonath A, Glotz C, Gewitz HS, Bartels K, von Böhlen K, Makowski I, Wittmann HG (1988) Characterization of crystals of small ribosomal subunits. J Mol Biol 203:831–834

Yonath A, Bennett W, Weinstein W, Wittmann HG (1990) Crystallography and image reconstruction of ribosomes. In: Hill EW, Dahlberg A, Garrett RA, Moore PB, Schlesinger D, Warner JR (eds) The ribosomes, structure, function and evolution. Am Soc Microbiol, Washington, pp 134–147

Yusupov MM, Tischenko SV, Trackhanov SD, Ryazantsev SN, Garber MB (1988) A new crystalline form of 30S ribosomal subunits from *Thermus thermophilus*. FEBS Lett 238, 113:115

Zamir A (1977) Affinity Labeling of ribosomal functional sites. Meth Enzymol 46:621–711